Calculation of electron-impact total-ionization cross sections

Philip L. Bartlett* and Andris T. Stelbovics†
Centre for Atomic, Molecular and Surface Physics, School of Mathematical and Physical Sciences, Murdoch University, Perth 6150, Australia

(Received 20 February 2002; revised manuscript received 12 April 2002; published 19 July 2002)

A computationally efficient analytic form of the Born-approximation electron-impact ionization amplitude is derived for general neutral-atom targets. High-quality Hartree-Fock Slater orbitals are used to model the target wave function. Full orthogonalization of the continuum Coulomb wave to all occupied orbitals of the target atom is enforced. Results are presented for noble gases (Ne, Ar, Kr, and Xe), selected transition metals (Fe, Cu, and Ag), and elements from the fourth, fifth, and sixth columns of the periodic table (Si, Ge, Sn, P, As, Sb, S, Se, and Te), where theoretical comparisons are lacking. Full orthogonalization significantly improves agreement with experimental data for the noble-gas series compared to previous Born models. Overall agreement with all elements is uniformly good and variations within each series are systematic.

DOI: 10.1103/PhysRevA.66.012707 PACS number(s): 34.80.Dp, 03.65.Nk, 13.85.Hd, 31.15.−p

I. INTRODUCTION

There has been a significant amount of research in recent decades into improving the theory of electron-impact ionizing collisions with atoms and ions. Though the interactions between the fundamental particles are known, the intractability of the resulting mathematical equations has led to many types of approximations and methods, in order to obtain solutions.

To date, the convergent close-coupled (CCC) methodology of Bray and Stelbovics (see Ref. [1] for a general discussion of this method) has provided the best correlation of scattering theory with experimental results. However, this method is computationally intensive and is currently limited to the valence shell of atoms containing only one or two valence electrons. Recent work by Baertschy *et al.* [2] has described the exterior complex scaling (ECS) method, which requires massively parallel supercomputing to solve the three-body problem without significant approximation. This has provided very accurate theoretical results for hydrogen at low incident energies, but will require significant advances in computing technology before it can be applied to larger atoms.

On the other hand, there exists a comprehensive set of recent measurements by Freund *et al.* [3], Shah *et al.* [4], Bolorizadeh *et al.* [5], and others, for accurate relative and absolute total ionization cross sections of many of the heavier atoms and ions, including the transition metals. There have also been continued experimental measurements for the noble gases including those of Sorokin *et al.* [6] and Wetzel *et al.* [7]. So for these atoms, experimentalists had to rely upon less sophisticated Born-approximation calculations for comparison with their results when they were available.

The Born approximation for ionizing collisions is, in contrast to CCC, less computationally intense and had many variants over recent decades. It is still regularly cited in experimental and theoretical publications and surprisingly for some target data, no theoretical calculations, including Born models, have been reported in the literature.

Early attempts at using Born approximations were known to result in overestimations of the ionization cross sections near their maximum (see, for example, the work of Peach [8]). This was due to the use of a hydrogenic Coulomb wave to describe the ejected continuum electron, which was not orthogonal to the target state orbitals. Omidvar *et al.* [9] and McCarthy and Stelbovics [10] provided analytic expressions for the Born triple-differential cross section (TDCS) using plane waves for the incident and scattered electrons and a Coulomb wave of unit charge for the ejected electron; in both approaches the Coulomb wave function was orthogonalized to the target atomic orbital of the ejected electron. Omidvar *et al.* [9] used screened hydrogenic wave functions, with screening parameters obtained from Hartree-Fock calculations, whereas McCarthy and Stelbovics [10] used the higher-quality Hartree-Fock Slater functions of Clementi and Roetti [11] to model the target states. The latter approach provided a better model for the target wave functions, but was limited to *s* and *p* orbitals.

A different variant of the Born approximation was employed by McGuire [12,13]. It was based upon expansion techniques where the active electron is in a Coulomb potential of variable charge. This charge is approximated by a series of straight lines, fitted to a theoretical calculation of the generalized oscillator strength for the target atom. McGuire published results for a large range of atoms, which appear to give good correlation to experimental data at high energies, but as we will see in Sec. III, these are not consistently good at low energies and mid energies. His calculations constitute the most detailed study of trends across the periodic table in the literature.

The method presented here is based upon the work of McCarthy and Stelbovics [10], but extended to provide an analytic solution for atomic orbitals with *arbitrary* angular momentum. Also, the Coulomb wave has been made orthogonal to *all* occupied atomic orbitals, which, as will be demonstrated, provides a significant improvement over the calculations of Omidvar *et al.* [9], McGuire [12,13], and McCarthy and Stelbovics [10], for many of the atoms consid-

*Electronic address: bartlett@fizzy.murdoch.edu.au
†Electronic address: stelbovi@fizzy.murdoch.edu.au

ered. The feature of our study is that a comprehensive set of targets is studied within the same theoretical framework using high-quality target states and with full orthogonalization of the continuum ejected electron, thus enabling trends across the periodic table to be examined and compared with those of McGuire's investigations. The results reported in this paper demonstrate that our procedure provides consistently good high-energy approximations for *all* atoms, and significantly reduced deviations from experiment near the cross-section maxima.

II. THEORY

In the case of the electron-impact ionization of a target atomic orbital, the Born approximation is given by Landau and Lifshitz [14] (in atomic units) as

$$d\sigma = \frac{4k'\kappa^2}{kq^4} |(e^{-i\mathbf{q}\cdot\mathbf{r}})_{nlm\,\boldsymbol{\kappa}}|^2 d\Omega d\Omega_\kappa d\kappa, \tag{1}$$

where σ is the ionization cross section, $d\Omega$ and $d\Omega_\kappa$ are elements of solid angle about the scattered and ejected electrons, respectively, n, l, and m are the usual orbital, angular momentum, and magnetic quantum numbers, $\boldsymbol{k}$ is the incident electron momentum (directed along the positive $\boldsymbol{z}$ axis), $\boldsymbol{k}'$ is the scattered electron momentum, $\boldsymbol{\kappa}$ is the ejected electron momentum, and $\boldsymbol{q}=\boldsymbol{k}-\boldsymbol{k}'$ is the momentum transfer. The matrix element is given as

$$(e^{-i\mathbf{q}\cdot\mathbf{r}})_{nlm\,\boldsymbol{\kappa}} = \int \psi_{\boldsymbol{\kappa}}^{(-)*} e^{-i\mathbf{q}\cdot\mathbf{r}} \phi_{nlm} d^3r, \tag{2}$$

where ϕ_{nlm} is the target orbital wave function and $\psi_{\boldsymbol{\kappa}}^{(-)}$ is the ejected electron wave function.

To evaluate Eq. (1), all momenta in the equation must be expressed in terms of the known variables and the integration variables. These are given by

$$k = \sqrt{2E}, \tag{3}$$

$$k' = \sqrt{2(E - E_0 - \kappa^2/2)}, \tag{4}$$

$$q = k^2 + k'^2 - 2kk' \cos\theta, \tag{5}$$

where E is the incident electron energy, E_0 is the ionization energy of the target orbital, and θ is the angle between $\boldsymbol{k}'$ and the $\boldsymbol{z}$ axis.

The total-ionization cross section (TICS) of an atom is the sum of the ionization cross sections of each of the occupied orbitals,

$$\sigma = \sum_{nlm} \frac{N_{nl}\sigma_{nlm}}{2l+1}, \tag{6}$$

where N_{nl} is the number of electrons in the nl orbital and it is assumed that the electrons are equally shared amongst the available m quantum states.

The incident and ejected electrons are identical particles but no allowance has been made in Eq. (1) for particle exchange. To compensate for this omission, the upper integration limit of the $\boldsymbol{\kappa}$ momentum integration is taken to be $\sqrt{k^2/2 - E_0}$, which is the momentum of an electron ejected with half of the maximum possible energy. This so-called Born-B approximation will always yield better results when, as is usually the case, the effects of exchange are to reduce the cross section [15].

The Roothaan-Hartree-Fock calculations of Clementi and Roetti [11] have been used to approximate the wave functions of the occupied orbitals of the target atom. The wave function for a single atomic orbital is presented as a sum of Slater functions,

$$\phi_{nlm}(r,\theta,\phi) = \sum_\mu c_\mu A_\mu r^{n_\mu - 1} e^{-\lambda_\mu r} Y_{lm}(\theta,\phi), \tag{7}$$

where $Y_{lm}(\theta,\phi)$ is a spherical harmonic and

$$A_\mu = [(2n_\mu)!]^{-1/2} (2\lambda_\mu)^{n_\mu + 1/2}. \tag{8}$$

The outgoing scattered electron is described by a plane wave, and the ejected electron is modeled by the hydrogenic Coulomb wave function, which (normalized to the three-dimensional δ function in momentum space) is given by

$$\psi_{\boldsymbol{\kappa}}^{(-)} = \frac{1}{(2\pi)^{3/2}} e^{\pi/2\kappa} \Gamma(1 + i/\kappa) e^{i\boldsymbol{\kappa}\cdot\mathbf{r}} \times {}_1F_1(-i/\kappa, 1, -i\kappa r - i\boldsymbol{\kappa}\cdot\mathbf{r}). \tag{9}$$

Here Γ is the gamma function, ${}_1F_1$ is the confluent hypergeometric function, and $\boldsymbol{\kappa}$ is the momentum of the ejected electron.

Omidvar *et al.* [9] used screened hydrogenic wave functions in place of the Slater functions in Eq. (7), and parabolic coordinates (and the completeness relation over these coordinates) to find an analytic expression for their final ionization amplitude. However, in a similar approach to that of McCarthy and Stelbovics [10], we employ spherical-polar coordinates throughout, and begin by using the well-known closed-form solution to the matrix element for the ground state of hydrogen, given by

$$(e^{-i\mathbf{q}\cdot\mathbf{r}})_{1s\,\boldsymbol{\kappa}} = \frac{\sqrt{2}}{\pi} \Gamma(1 + i\xi) e^{\pi\xi/2} \left(\frac{-\partial}{\partial\lambda} \frac{A^{-i\xi}}{B^{1-i\xi}} \right)\Bigg|_{\lambda=1}, \tag{10}$$

where, for a target with total charge $+1$ (after ionization),

$$\xi = 1/\kappa, \tag{11}$$

$$A = q^2 - (\kappa + i\lambda)^2, \tag{12}$$

$$B = |\boldsymbol{q} + \boldsymbol{\kappa}|^2 + \lambda^2 = q^2 + \kappa^2 + 2\boldsymbol{q}\cdot\boldsymbol{\kappa} + \lambda^2. \tag{13}$$

McCarthy and Stelbovics also gave the analytic solution for the matrix element for s and p orbitals by using a first-order tensor form for the spherical harmonic, and applying parametric-integration techniques to solve the resulting equation.

In order to find a general solution for all orbitals we begin by deriving a first-order tensor representation of the spherical harmonic function that is valid for all values of angular mo-

mentum. The Cartesian-coordinate representation for the spherical harmonic function is given, for $m \geqslant 0$, as [16]

$$Y_{lm}(\hat{\boldsymbol{r}}) = \left(\frac{2l+1}{4\pi} (l+m)!(l-m)! \right)^{1/2} r^{-l} \times \sum_{k=0}^{\lfloor (l-m)/2 \rfloor} \left(\frac{(-x-iy)^{k+m}(x-iy)^k z^{l-m-2k}}{2^{2k+m}(k+m)!k!(l-m-2k)!} \right). \tag{14}$$

Substituting the first-order tensors,

$$r_{+1} = \frac{-x-iy}{\sqrt{2}}, \quad r_0 = z, \quad r_{-1} = \frac{x-iy}{\sqrt{2}}, \tag{15}$$

where x, y, and z are the usual Cartesian coordinates, into Eq. (14) and using the relationship

$$Y_{lm}(\hat{\boldsymbol{r}}) = (-1)^m Y_{l-m}^*(\hat{\boldsymbol{r}}), \tag{16}$$

the general form for the spherical harmonic in first-order tensors becomes

$$Y_{lm}(\hat{\boldsymbol{r}}) = r^{-l} \sum_{k=0}^{\lfloor (l-|m|)/2 \rfloor} \alpha_{klm} r_0^{\beta_0} r_1^{\beta_1} r_{-1}^{\beta_{-1}}, \tag{17}$$

where

$$\alpha_{klm} = \frac{\left[\frac{2l+1}{4\pi} (l+m)!(l-m)! \right]^{1/2}}{2^{k+|m|/2}(k+|m|)!k!(l-|m|-2k)!}, \tag{18}$$

$$\beta_0 = l - |m| - 2k, \tag{19}$$

$$\beta_1 = \begin{cases} k+m, & m \geqslant 0 \\ k, & m < 0, \end{cases} \tag{20}$$

$$\beta_{-1} = \begin{cases} k, & m \geqslant 0 \\ k-m, & m < 0. \end{cases} \tag{21}$$

It should be noted that $\beta_{-1} + \beta_0 + \beta_1 = l$.

Now, to solve the matrix-element equation (2), we substitute Eqs. (17) and (7), giving

$$(e^{-i\boldsymbol{q}\cdot\boldsymbol{r}})_{nlm\,\boldsymbol{\kappa}} = \int \psi_{\boldsymbol{\kappa}}^{(-)*} e^{-i\boldsymbol{q}\cdot\boldsymbol{r}} \sum_\mu c_\mu A_\mu r^{n_\mu - l - 1} \times e^{-\lambda_\mu r} \sum_{k=0}^{\lfloor (l-|m|)/2 \rfloor} \alpha_{klm} r_0^{\beta_0} r_1^{\beta_1} (r_{-1})^{\beta_{-1}} d^3 r, \tag{22}$$

which by rearranging, simplifying, and using parametric integration simplifies to

$$(e^{-i\boldsymbol{q}\cdot\boldsymbol{r}})_{nlm\,\boldsymbol{\kappa}} = \sum_\mu c_\mu A_\mu \left(\frac{-\partial}{\partial \lambda_\mu} \right)^{(n_\mu - l)} \sum_{k=0}^{\lfloor (l-|m|)/2 \rfloor} \alpha_{klm} \times \int r_0^{\beta_0} r_1^{\beta_1} (r_{-1})^{\beta_{-1}} \psi_{\boldsymbol{\kappa}}^{(-)*} e^{-i\boldsymbol{q}\cdot\boldsymbol{r} - \lambda_\mu r} \frac{d^3 r}{r}. \tag{23}$$

The tensors can be removed from within the integral by taking advantage of the relationship

$$(r_a r_b \cdots) e^{-i\boldsymbol{q}\cdot\boldsymbol{r}} \equiv \left(i \frac{\partial}{\partial q_a^*} \right) \left(i \frac{\partial}{\partial q_b^*} \right) (\cdots) e^{-i\boldsymbol{q}\cdot\boldsymbol{r}}, \tag{24}$$

where, as usual, $*$ represents conjugation, and the q tensors are defined in terms of their Cartesian components as given by Eq. (15). Then, converting the remaining integral to a form similar to that used in Eq. (10) yields

$$W_{nlm}(\boldsymbol{q}, \boldsymbol{\kappa}) = (e^{-i\boldsymbol{q}\cdot\boldsymbol{r}})_{nlm\,\boldsymbol{\kappa}}^{\text{no orthog}} = \left(\frac{2}{\pi} \right)^{1/2} i^l \Gamma(1 + i\xi) e^{\pi\xi/2} \times \sum_\mu c_\mu A_\mu \left\{ \left(\frac{-\partial}{\partial \lambda_\mu} \right)^{(n_\mu - l)} \sum_{k=0}^{\lfloor (l-|m|)/2 \rfloor} \alpha_{klm} \times \left(\frac{\partial^{(l)}}{\partial^{(\beta_0)} q_0^* \partial^{(\beta_1)} q_1^* \partial^{(\beta_{-1})} q_{-1}^*} \right) \frac{A^{-i\xi}}{B^{1-i\xi}} \right\}. \tag{25}$$

To solve Eq. (25), the following tensor relations were used:

$$q^2 = q_0^{*2} - 2 q_1^* q_{-1}^*, \tag{26}$$

$$\boldsymbol{q}\cdot\boldsymbol{\kappa} = q_0^* \kappa_0 + q_1^* \kappa_1 + q_{-1}^* \kappa_{-1}. \tag{27}$$

As expected, Eq. (25) simplifies to Eq. (10) for $l = 0$, and we arrived at the general solution of the matrix-element equation.

The Coulomb wave function $\psi_{\boldsymbol{\kappa}}^{(-)}$ is not orthogonal to the Hartree-Fock orbital wave functions, but Omidvar *et al.* [9] demonstrated that forcing $\psi_{\boldsymbol{\kappa}}^{(-)}$ to be orthogonal to the active electron wave function will improve the resulting cross section. However, in this application we orthogonalize $\psi_{\boldsymbol{\kappa}}^{(-)}$ to not only the target orbital wave function, but all occupied orbitals of the target atom.

The fully orthogonalized Coulomb wave function is given by

$$\psi_{\boldsymbol{\kappa}\,\text{orthog}}^{(-)} = \psi_{\boldsymbol{\kappa}}^{(-)} - \sum_{n'l'm'} \phi_{n'l'm'} \langle \phi_{n'l'm'}^* | \psi_{\boldsymbol{\kappa}}^{(-)} \rangle, \tag{28}$$

where the $n'l'm'$ summation includes all orbitals for which the Coulomb wave function is required to be made orthogonal. This relation is only applicable if the $\phi_{n'l'm'}$ wave functions form an orthonormal set, which is the case with the wave functions presented by Clementi and Roetti [11]. This

equation is used in place of $\psi_{\boldsymbol{\kappa}}^{(-)}$ in the matrix-element equation (2), and the fully orthogonalized matrix element simplifies to

$$(e^{-i\boldsymbol{q}\cdot\boldsymbol{r}})_{nlm\ \boldsymbol{\kappa}} = W_{nlm}(\boldsymbol{q},\boldsymbol{\kappa}) - \sum_{n'l'm'} F_{ll'mm'}(\boldsymbol{q}) \times W_{n'l'm'}(\boldsymbol{0},\boldsymbol{\kappa}), \tag{29}$$

where $n'l'm'$ sums over all occupied orbitals, and where

$$F_{ll'mm'}(\boldsymbol{q}) = \sum_{\mu\mu'} c_\mu c_{\mu'} A_\mu A_{\mu'} \int r^{n_\mu + n_{\mu'} - 2} \times e^{-i\boldsymbol{q}\cdot\boldsymbol{r} - (\lambda_\mu + \lambda_{\mu'})r} Y_{lm}^* Y_{l'm'} d^3r. \tag{30}$$

In order to compute the integral, we substitute the general spherical harmonic (17) into Eq. (30) and use the spherical harmonic conjugate relationship (16) to give

$$F_{ll'mm'}(\boldsymbol{q}) = 8\pi(-1)^m i^{l+l'} \sum_{\mu\mu'} c_\mu c_{\mu'} A_\mu A_{\mu'} \left(\frac{-\partial}{\partial\lambda}\right)^{N-l-l'} \left\{ \lambda \left[\left(\sum_{k=0}^{[(l-|m|)/2]} \alpha_{klm} \frac{\partial^{(l)}}{(\partial^{(\beta_0)} q_0^*)(\partial^{(\beta_{-1})} q_1^*)(\partial^{(\beta_1)} q_{-1}^*)} \right) \times \left(\sum_{k'=0}^{[(l'-|m'|)/2]} \alpha_{k'l'm'} \frac{\partial^{(l')}}{(\partial^{(\beta_0')} q_0^*)(\partial^{(\beta_1')} q_1^*)(\partial^{(\beta_{-1}')} q_{-1}^*)} \right) \right] \left(\frac{1}{(\lambda^2+q^2)^2} \right) \right\}, \tag{31}$$

where β_m are as defined previously and

$$N = n_\mu + n_{\mu'} - 2, \tag{32}$$

$$\lambda = \lambda_\mu + \lambda_{\mu'}, \tag{33}$$

$$\beta_0' = l' - |m'| - 2k', \tag{34}$$

$$\beta_1' = \begin{cases} k'+m', & m' \geqslant 0 \\ k', & m' < 0, \end{cases} \tag{35}$$

$$\beta_{-1}' = \begin{cases} k', & m' \geqslant 0 \\ k'-m', & m' < 0. \end{cases} \tag{36}$$

These equations are well suited to algebraic computing, and were used to develop a Maple procedure that calculated the analytic form for the TDCS for all atoms considered by Clementi and Roetti (He-Xe).

It should be noted that the final form of the TDCS equation has no ϕ dependence and the numerical integrations may be performed using $d\Omega_\kappa = 2\pi \sin\gamma$, where γ is the angle between the $\boldsymbol{q}$ and $\boldsymbol{\kappa}$, and $d\Omega = 2\pi \sin\theta$.

Maple was also used to convert the resulting equation into FORTRAN, which was linked with a three-dimensional Clenshaw-Curtis integration algorithm to calculate the total-ionization cross section. Our ionization cross sections at all energies and for all targets below have been computed to an accuracy of four significant figures.

III. RESULTS

In this section we will present results for a selection of noble gases, transition metals, and selected elements from the fourth, fifth, and sixth columns of the periodic table. This selection has been made on the basis of recent experimental interest. In addition to the results presented here we can supply (upon request) calculated results for any neutral target up to and including xenon. The ionization energy E_0 used to calculate the valence-shell ionization cross sections has been taken from experimental measurements [17]. Typically, the valence orbital energy of the Clementi and Roetti [11] Hartree-Fock calculations is between 0 eV and 1 eV, which is higher (less negative) than the experimental values. Using the latter lowers the peak cross section by up to 10%, and provides better alignment with the near-threshold experimental results, while the high-energy results remain unchanged.

Where experimental results are presented for single-, double-, and triple-ionization cross sections, only the single-ionization results are compared to the theoretical calculations.

As the Born approximation is known to be accurate at high energies, a high-energy graph is also presented for each element so that convergence with other theoretical and experimental results can be examined more closely.

A. Noble gases

To date, the experimental results of the noble gases (except He) have exhibited a significant variation from quantum-mechanical calculations. Sorokin *et al.* [6,21] have performed a detailed analysis of experimental and theoretical TICS for Ne and Ar, showing that the theoretical results of McGuire [12,13] exhibit the best high-energy convergence with experimental data for both elements, while all quantum-mechanical results for Ar overestimate significantly (>50%) the peak cross section.

The results of Sorokin *et al.* [6,21] have been normalized by comparison with photoionization cross sections while the results of McCallion *et al.* [22] were normalized to the absolute measurements of Rapp and Englander-Golden [23]. The results of Freund *et al.* [3] and Wetzel *et al.* [7] were absolute measurements.

Figures 1(a) and 1(b) for neon show that by extending the orthogonalization of the Coulomb wave function to all occu-

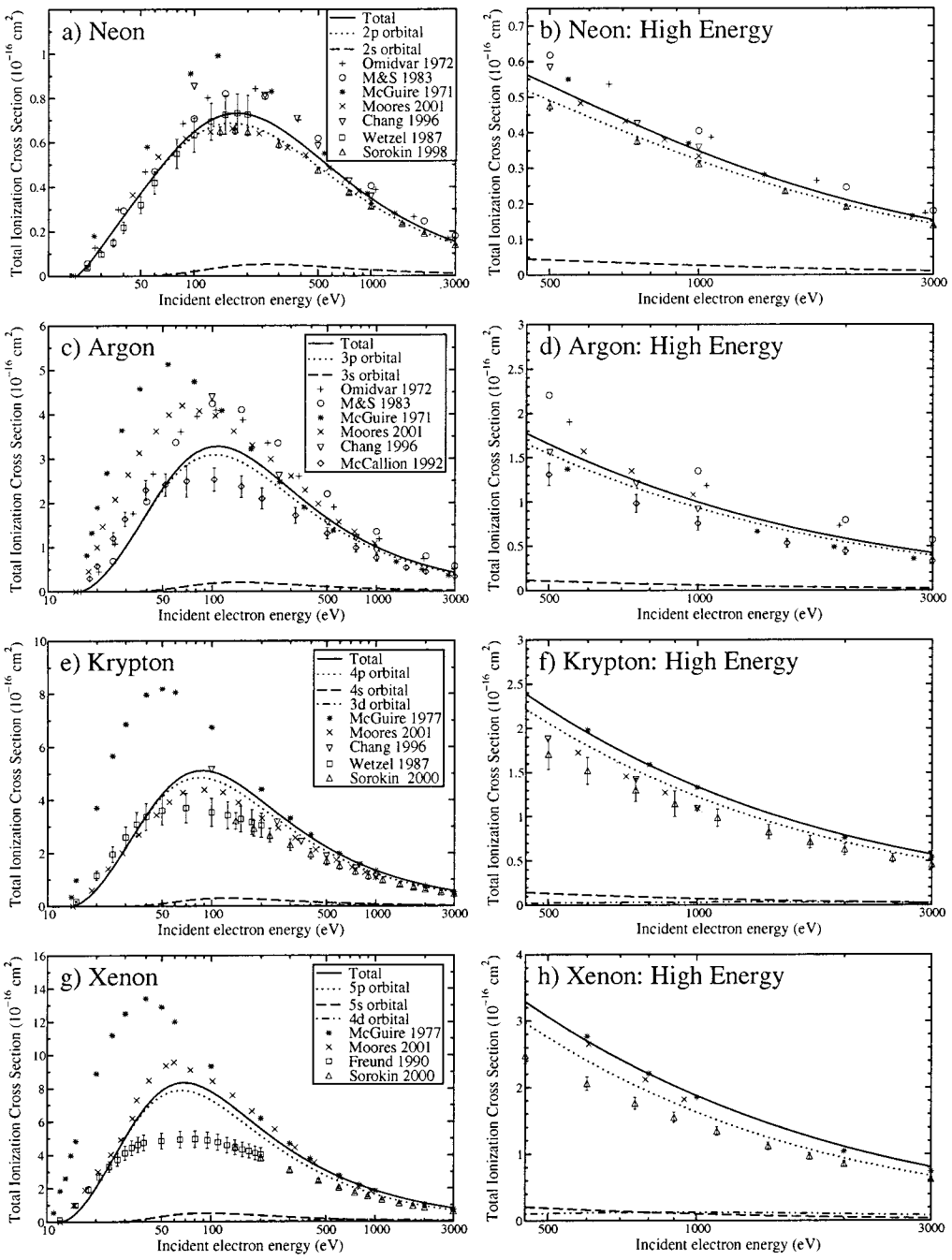

FIG. 1. Total electron-impact ionization cross section for the noble gases Ne, Ar, Kr, and Xe. The present TICS calculations are displayed with full dark lines and the TICS for the major component orbitals are displayed with broken lines. Other theoretical calculations are by Omidvar *et al.* [9], McCarthy and Stelbovics [18], McGuire [12,13], Moores [19], and Chang and Altick [20]. Experimental results are by Wetzel *et al.* [7], Sorokin *et al.* [6,21], McCallion *et al.* [22], and Freund *et al.* [3], and have error bars indicating their absolute uncertainty.

pied orbitals, the TICS has been moderately reduced at mid-to-high energies, by comparison with the results of McCarthy and Stelbovics [10], using orthogonalization against the ionized orbital only. Though Omidvar *et al.* [9] and McCarthy and Stelbovics used different atomic wave functions, their results were very similar. Recent distorted-wave calculations of Chang and Altick [20] and Moores [19] are also included for comparison. Chang and Altick's results, at the lowest energy in the limited range, are similar to those of McGuire [12].

At high energies, the present calculations are in excellent agreement with those of McGuire (to within 1%), Chang and Altick, and Moores, and good agreement was obtained with the experimental results of Sorokin *et al.* [21] (to within 10%). At low energies, our calculations show significant improvement over McGuire, and are in reasonable agreement with both sets of experimental data. However, Moores' calculations are slightly closer to experiment at low-to-mid energies. Overall, the present calculations for neon are within 10% of experimental values at all energies above 50 eV.

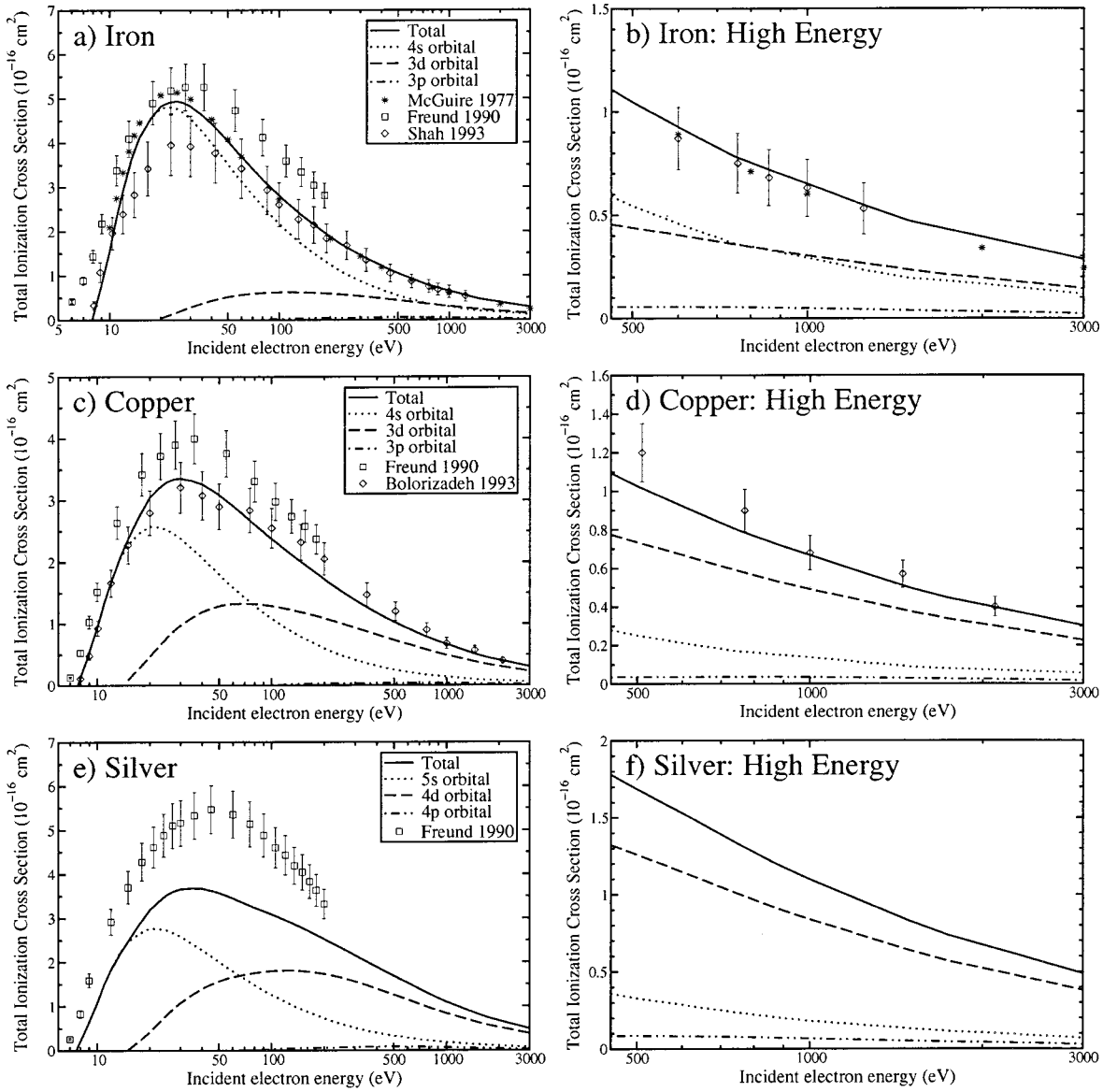

FIG. 2. Total electron-impact ionization cross section for the transition metals Fe, Cu, and Ag. Theoretical calculations are by McGuire [13] and experimental results by Freund *et al.* [3], Shah *et al.* [4], and Bolorizadeh *et al.* [5]. See Fig. 1 for further details.

Figures 1(c) and 1(d) for argon show a more pronounced improvement due to full orthogonalization, and a large improvement over the results of McGuire [12] at low energies. Both Chang and Altick [20] and Moores [19] agree closely with us on the high-energy side of the cross section. At the highest energies [Fig. 1(d)] McGuire agrees with the data of McCallion *et al.* [22], within experimental error. This was the only noble gas where the present calculations differed significantly from McGuire at high energies. The argon data for McGuire was obtained from Fig. 11 of his 1971 paper [12] whereas the remaining noble-gas cross sections were extracted from his tables [12,13]. However, as the data of McCallion *et al.* were normalized against relatively old absolute measurements, conclusions on the accuracy of the high-energy results cannot be made with certainty. At low-to-mid energies our calculations were significantly closer to experiment than the calculations of Chang and Altick and Moores. Overall, the present calculations for argon are within 30% of experimental values at all energies above 50 eV.

Figures 1(e,f) and 1(g,h) for krypton and xenon, respectively, show similar improvements over McGuire [13]. However, the deviation from experimental results increases with increasing atomic number, being up to 40% for krypton and 70% for xenon near the cross-section peaks. It is worth noting that for krypton, the close correlation between the results of McGuire and Chang and Altick [20] are no longer evident. The Chang and Altick data near the maximum of the peak are very close to our calculation and at high energies their results trend slightly below those of McGuire and us, which are in excellent agreement with each other. Moores' [19] calculations for krypton are slightly closer to experiment than our calculations for all energies, but are slightly further from experiment at the peak cross section for xenon.

In summary, for Ar, Kr, and Xe the energies of the peak cross section align more closely with the experimental re-

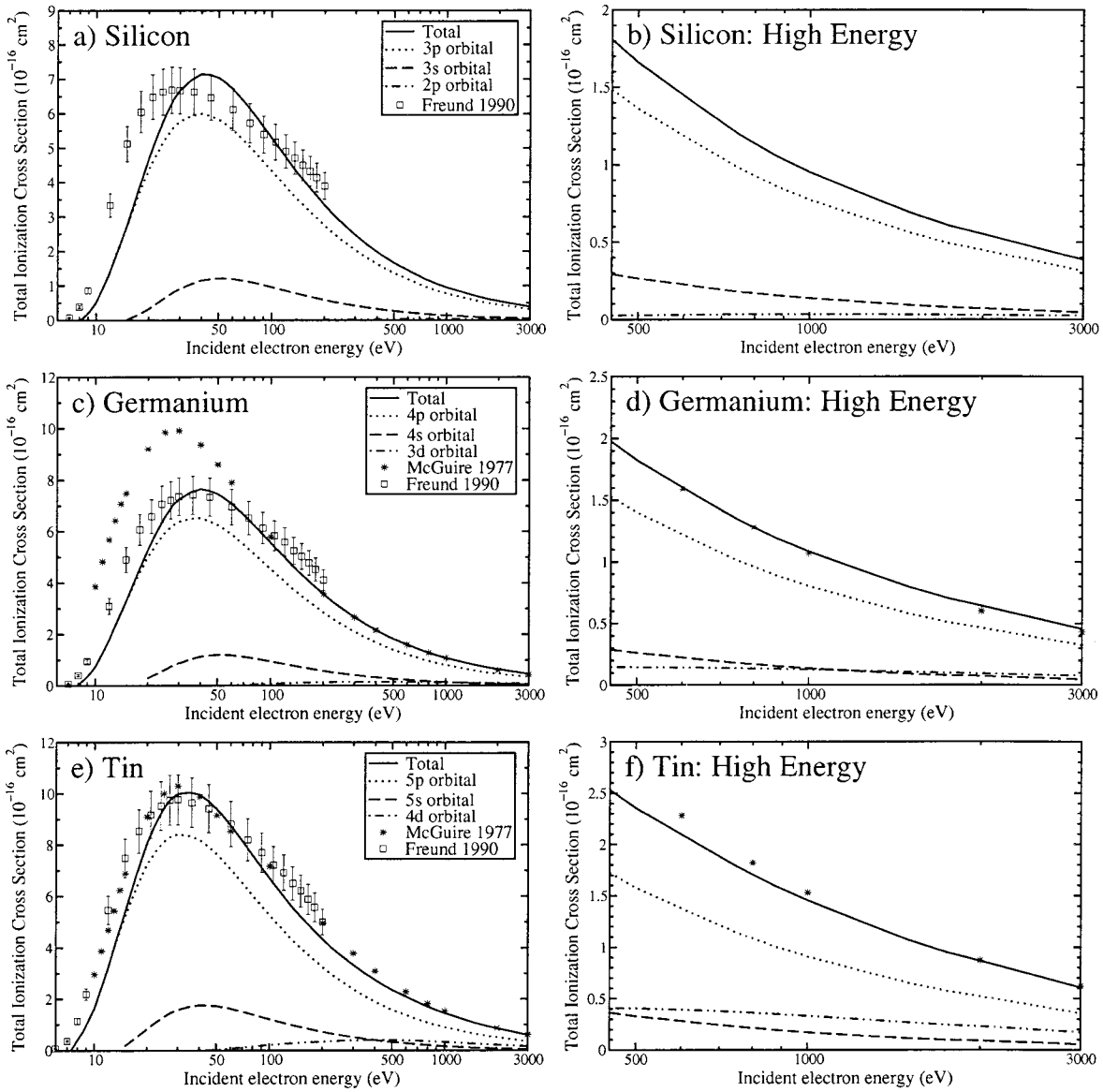

FIG. 3. Total electron-impact ionization cross section for the fourth-column elements Si, Ge, and Sn. Theoretical calculations are by McGuire [13] and experimental results by Freund *et al.* [3]. See Fig. 1 for further details.

sults than those of McGuire, and for all noble gases presented, the low-energy cross sections show a significant improvement. With the exception of argon, our calculations are in good agreement with the recent distorted-wave calculations of Moores. We note that his calculations include interaction between the incident and scattered particles and the target, and also have allowance for electron exchange. His model is thus more sophisticated than ours, which does not include such effects apart from an approximate allowance for exchange. It seems therefore, that there is a considerable averaging over all these effects at lower energies for the noble gases, enabling our Born model to provide good estimates for the total-ionization cross sections.

B. Transition metals

Figures 2(a) and 2(b) for iron show excellent agreement with McGuire [13] at all energies, and excellent agreement with the results of Shah *et al.* [4] at high energies. It should be noted that the results of Shah *et al.* were not absolute measurements, but were normalized by comparing their double-ionization cross-section results with those of Freund *et al.* [3]. Normalization to the double-ionization cross section was chosen because the single-ionization results of Freund *et al.* were significantly affected by an admixture of low-lying metastable states in the target beam. This is evident from the TICS measurements obtained below the ionization threshold of 7.9 eV. However, this was not expected to affect their double-ionization results, and Shah *et al.* justified this by the close agreement of their high-energy results with McGuire. The present calculations confirm the validity of this normalization procedure, and are well within experimental error for energies above 50 eV.

Figures 2(c) and 2(d) for copper demonstrate excellent agreement with Bolorizadeh *et al.* [5], being within experi-

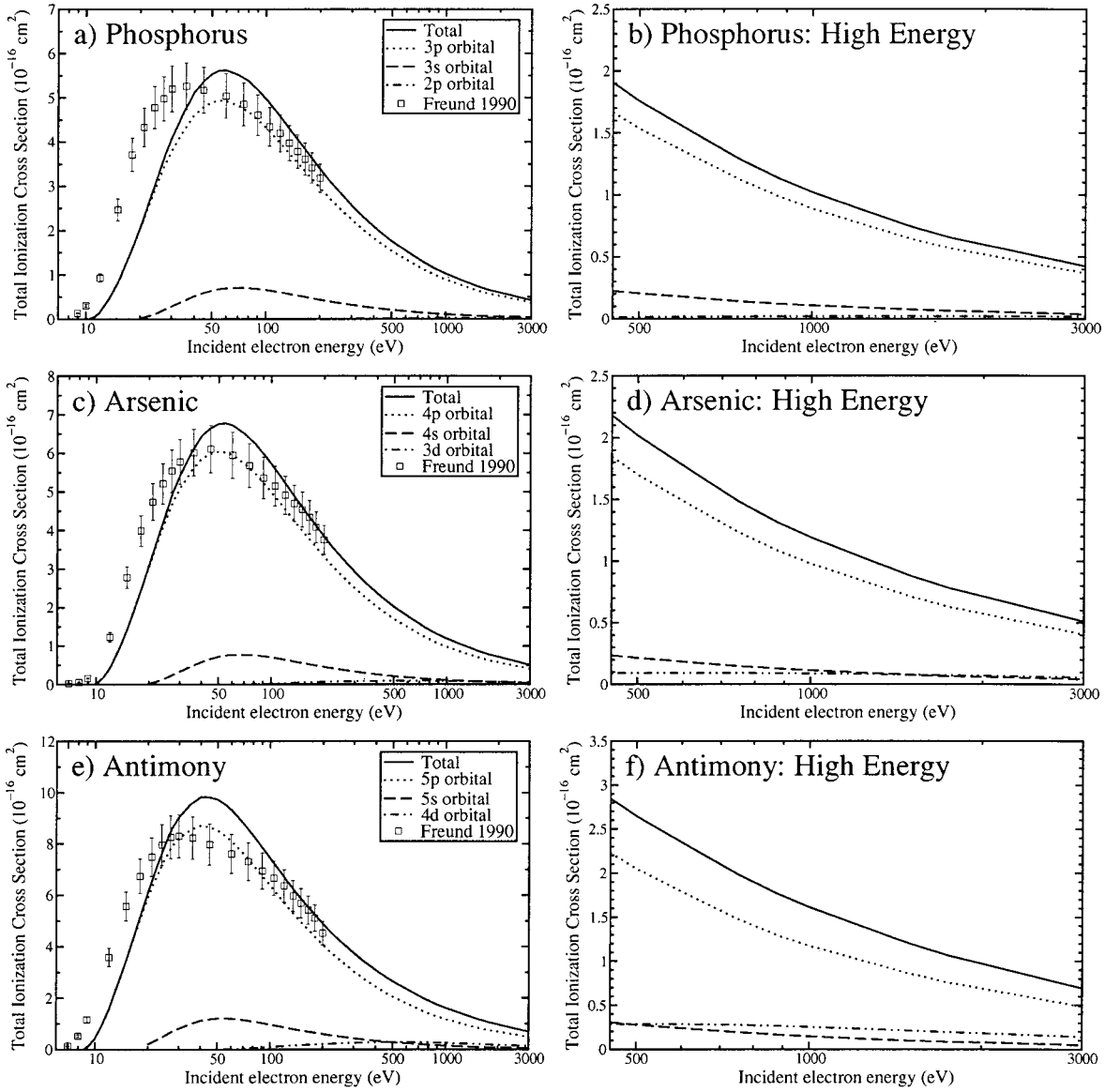

FIG. 4. Total electron-impact ionization cross section for the fifth-column elements P, As, and Sb. Experimental results are by Freund *et al.* [3]. See Fig. 1 for further details.

mental error at all energies. The cross-section points below ionization threshold indicate that the Freund *et al.* results have been affected by an admixture of metastable states. Like iron, the results of Bolorizadeh *et al.* were normalized by comparing their double-ionization cross-section results with those of Freund *et al.* [3]. McGuire [13] only published the results of fourth and fifth row elements with an *even* atomic number, and no other theoretical calculations could be found.

Figures 2(e) and 2(f) for silver also demonstrate that Freund *et al.* [3] results were affected by metastable states, and by comparing the 7-eV measurement with that of copper, it appears that there is a larger population of these states. As no other published experimental results could be found for silver, we can only surmise that the elimination of metastable states would (as is the case for Fe and Cu) significantly reduce the TICS reported by Freund *et al.* If this reduction in TICS increases in proportion to the population of metastable states, then a larger reduction in TICS would be expected for silver than copper. This suggests that the present calculations may align reasonably well to experimental results that were free from admixtures of metastable states.

It is significant that for the transition metals examined, the first-inner-shell ionization occurs below the peak ionization cross section, and for Cu and Ag, this becomes the dominant contributor to the ionization cross sections at low energies ($<$80 eV). Present applications of CCC methods would permit the ionization cross section of the outer 4*s* and 5*s* orbitals of the transition metals to be calculated, but as their inner-shell ionization starts at very low energies, it limits the comparison of CCC with experiment to below approximately 15 eV. As our high-energy results for the transition metals correlate well with experiment, the present inner-shell ionization results could be coupled with future CCC valence-shell ionization results, to give improved low-to-mid-energy cross sections.

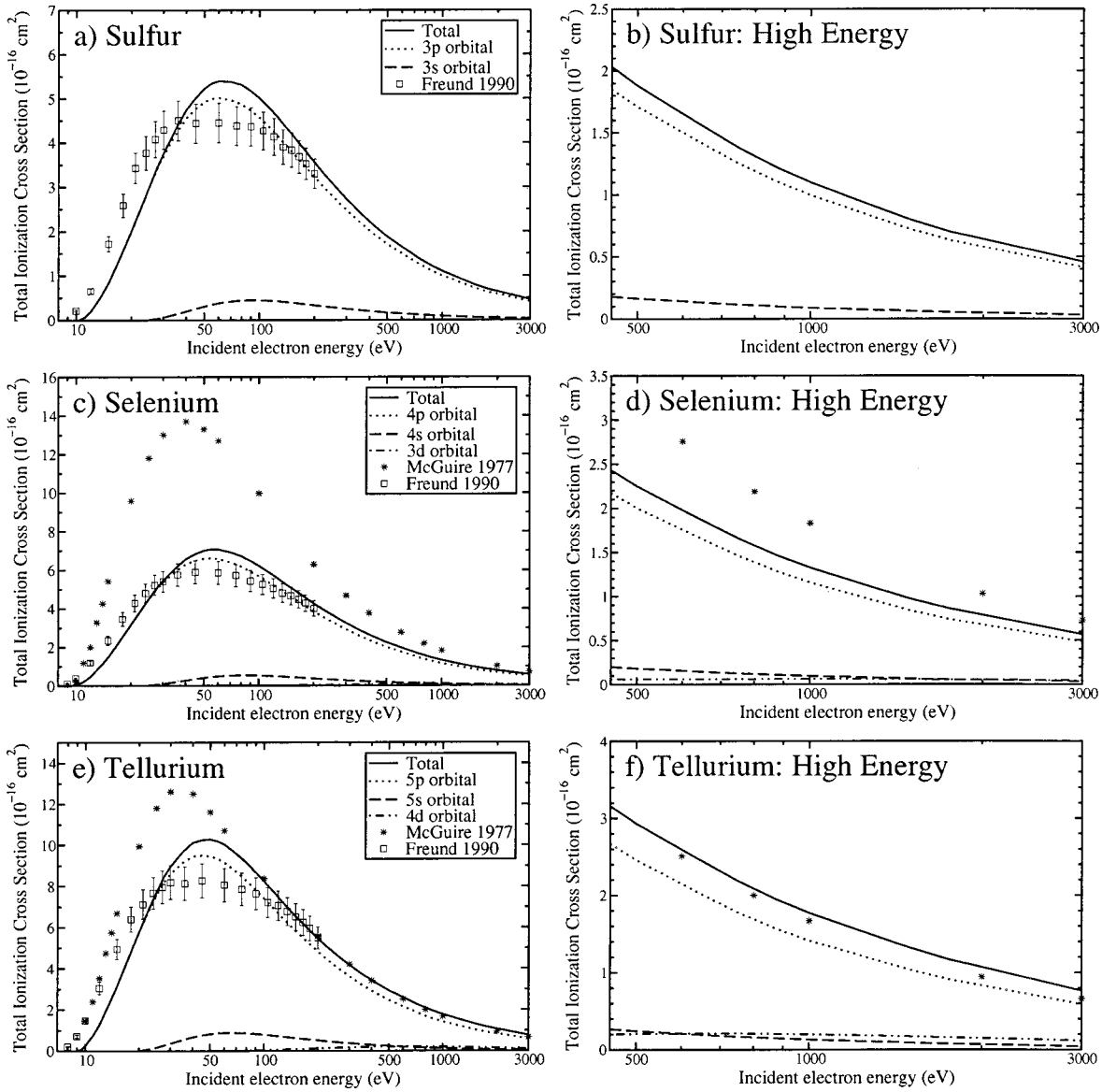

FIG. 5. Total electron-impact ionization cross section for the sixth-column elements S, Se, and Te. Theoretical calculations are by McGuire [13] and experimental results by Freund *et al.* [3]. See Fig. 1 for further details.

C. Fourth-, fifth-, and sixth-column elements

The elements selected in this section (with the exception of sulfur) are believed to have only experimental measurements performed by Freund *et al.* [3]. These data, like those of the transition metals, have been affected by an admixture of metastable states in the target beam, but perhaps to a lesser degree. Therefore, until subsequent experimental measurements are made, which are free from metastable states, a conclusive analysis of the accuracy of the present calculations cannot be made. Also, no high-energy experimental results are available for these elements, and only limited quantum-mechanical results are available.

Figure 3 shows the TICS for silicon, germanium, and tin. The present low-energy results are significantly lower than data of Freund *et al.* for each of these elements, but a large proportion of this difference is expected to be due to metastable states. There is good correlation with experiment at mid energies, with reasonable alignment of the peak cross sections.

Good high-energy convergence with McGuire [13] is obtained for germanium and tin, and the present low-energy results for germanium are significantly closer to experiment. Interestingly, McGuire's results for tin are in excellent agreement with ours at all energies whereas for germanium the typical overshoot at low energies compared to our calculation is evident.

Figure 4 shows the TICS for phosphorus, arsenic, and antimony. Our calculations show the same correlation with experiment as with the fourth-column elements. No other quantum-mechanical result can be found for these elements.

Figure 5 shows the TICS for sulfur, selenium, and tellurium. The present calculations show the same correlation with experiment as do the fourth- and fifth-column elements. The calculations for selenium show a dramatic improvement

over those of McGuire at low-to-mid energies, and only converge slowly to his calculations at high energies, with a 20% variation at 3000 eV being evident.

The experimental results for tellurium align more closely with McGuire at near-threshold energies. If corrections were made to the experimental results to compensate for the existence of metastable states, then they would be in better agreement with our calculations. The present calculations show an improvement over McGuire at energies close to the peak cross section and converge with McGuire in the 100–400 eV region. However, at higher energies they begin to diverge. The lack of high-energy experimental results prevents us from drawing any conclusion in this region.

IV. CONCLUSIONS

The Born model presented in Sec. II provides consistently good results for all the elements studied. It may be regarded as the maximal logical extension of the Born-amplitude approach. It combines the use of high-quality Hartree-Fock wave functions readily available in the literature with complete orthogonalization of the Coulomb continuum wave to all the target orbitals. The analytic amplitudes from this model can be integrated with high accuracy independent of the energy. The trends across the periodic table are remarkably consistent for the series examined and correlate extremely well with the most recent experimental data. Though there is still significant disagreement with the experimental results for the heavier noble gases, our calculations appear to be significantly better than previous quantum-mechanical Born ionization calculations and similar to the recent excellent distorted-wave calculations of Moores.

Preliminary calculations on the remaining columns of the periodic table also show encouraging results, and it is our future intention to publish tables for the electron-impact ionization cross sections for all the elements from hydrogen to xenon and for all orbitals.

The major improvement over previous calculations by Omidvar *et al.* [9], Peach [8], and McCarthy and Stelbovics [10], is provided by the orthogonalization of the ejected electron wave function against all occupied atomic orbitals. This has brought the ionization cross sections much closer to the experimental results at low-to-mid energies, and brought the high-energy results in better agreement with those of McGuire [12,13].

The methodology also allows evaluation of the ionization cross section of orbitals with any value of angular momentum. So it may be used to evaluate the *f*-orbital cross sections of the fifth- and sixth-column elements, or excited states of the lighter elements, subject to suitable Hartree-Fock calculations. Also, by providing an analytic solution to the TDCS equation (1), the method is not subject to errors introduced at high energies due to truncation of a partial-wave expansion.

ACKNOWLEDGMENTS

We wish to thank the Australian Research Council for supporting this work. One of us (P.L.B.) wishes to thank Murdoch University for providing funds that assisted this research.

[1] I. Bray and A. T. Stelbovics, Adv. At., Mol., Opt. Phys. **35**, 209 (1995).
[2] M. Baertschy, T. N. Rescigno, W. A. Isaacs, X. Li, and C. W. McCurdy, Phys. Rev. A **63**, 022712 (2001).
[3] R. S. Freund, R. C. Wetzel, R. J. Shul, and T. R. Hayes, Phys. Rev. A **41**, 3575 (1990).
[4] M. B. Shah, P. McCallion, K. Okuno, and H. Gilbody, J. Phys. B: At. Mol. Opt. Phys. **26**, 2393 (1993).
[5] M. A. Bolorizadeh, C. J. Patton, M. B. Shah, and H. B. Gilbody, J. Phys. B: At. Mol. Opt. Phys. **27**, 175 (1994).
[6] A. A. Sorokin, L. A. Shmaenok, S. V. Bobashev, B. Möbus, M. Richter, and G. Ulm, Phys. Rev. A **61**, 022723 (2000).
[7] R. C. Wetzel, F. A. Baiocchi, T. R. Hayes, and R. S. Freund, Phys. Rev. A **35**, 559 (1987).
[8] G. Peach, J. Phys. B **4**, 1670 (1971).
[9] K. Omidvar, H. L. Kyle, and E. C. Sullivan, Phys. Rev. A **5**, 1174 (1972).
[10] I. E. McCarthy and A. T. Stelbovics, Phys. Rev. A **28**, 1322 (1983).
[11] E. Clementi and C. Roetti, At. Data Nucl. Data Tables **14**, 177 (1974).
[12] E. J. McGuire, Phys. Rev. A **3**, 267 (1971).
[13] E. J. McGuire, Phys. Rev. A **16**, 62 (1977).
[14] L. D. Landau and E. M. Lifshitz, *Quantum Mechanics: Non-Relativistic Theory*, 2nd ed. (Pergamon, Reading, MA, 1965).
[15] M. R. H. Rudge, Rev. Mod. Phys. **40**, 564 (1968).
[16] J. D. Louck, in *Atomic, Molecular, & Optical Physics Handbook*, edited by G. W. F. Drake (AIP Press, New York, 1996), pp. 6–64.
[17] W. C. Martin and A. Musgrove, http://physics.nist.gov/PhysRefData/IonEnergy/ionEnergy.html (1999).
[18] I. E. McCarthy and A. T. Stelbovics (unpublished).
[19] D. L. Moores, Nucl. Instrum. Methods Phys. Res. B **179**, 316 (2001).
[20] D. W. Chang and P. L. Altick, J. Phys. B: At. Mol. Opt. Phys. **29**, 2325 (1996).
[21] A. A. Sorokin, L. A. Shmaenok, S. V. Bobashev, B. Möbus, and G. Ulm, Phys. Rev. A **58**, 2900 (1998).
[22] P. McCallion, M. B. Shah, and H. B. Gilbody, J. Phys. B: At. Mol. Opt. Phys. **25**, 1061 (1992).
[23] D. Rapp and P. Englander-Golden, J. Chem. Phys. **43**, 1464 (1965).